

# Analytical Methods

Accepted Manuscript

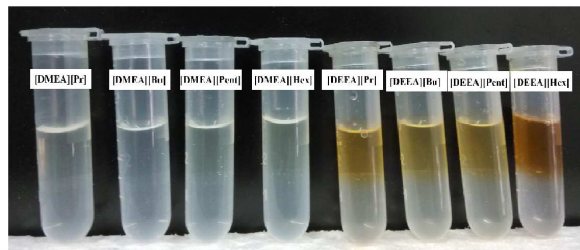
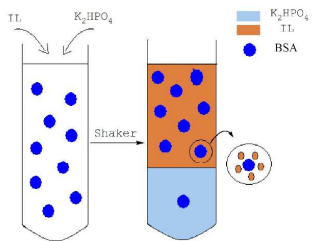


This is an *Accepted Manuscript*, which has been through the Royal Society of Chemistry peer review process and has been accepted for publication.

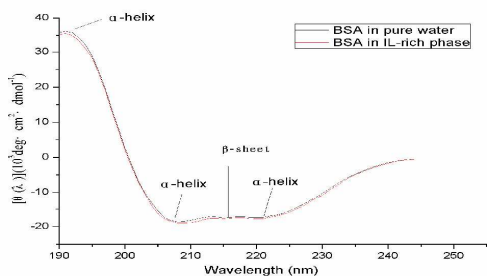
*Accepted Manuscripts* are published online shortly after acceptance, before technical editing, formatting and proof reading. Using this free service, authors can make their results available to the community, in citable form, before we publish the edited article. We will replace this *Accepted Manuscript* with the edited and formatted *Advance Article* as soon as it is available.

You can find more information about *Accepted Manuscripts* in the [Information for Authors](#).

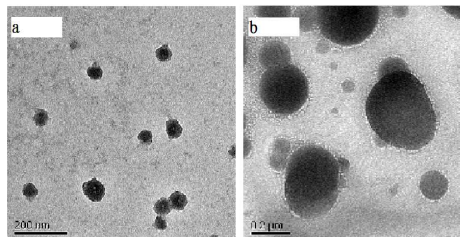
Please note that technical editing may introduce minor changes to the text and/or graphics, which may alter content. The journal's standard [Terms & Conditions](#) and the [Ethical guidelines](#) still apply. In no event shall the Royal Society of Chemistry be held responsible for any errors or omissions in this *Accepted Manuscript* or any consequences arising from the use of any information it contains.



select the optimal one from these ILs-ATPS



the circular dichroism spectra of protein



the TEM of before ILs-ATPS (a) and after (b)

1  
2  
3  
4  
5  
6  
7  
8  
9  
10  
11  
12  
13  
14  
15  
16  
17  
18  
19  
20  
21  
22  
23  
24  
25  
26  
27  
28  
29  
30  
31  
32  
33  
34  
35  
36  
37  
38  
39  
40  
41  
42  
43  
44  
45  
46  
47  
48  
49  
50  
51  
52  
53  
54  
55  
56  
57  
58  
59  
60

1  
2  
3  
4 1 **Partition of proteins with extraction in aqueous two-phase system by**  
5  
6 2 **hydroxyl ammonium-based ionic liquid**  
7

8  
9 3 Jing Chen, Yuzhi Wang\*, Qun Zeng, Xueqin Ding and Yanhua Huang  
10

11  
12  
13  
14 5 State Key Laboratory of Chemo/ Biosensing and Chemometrics, College of Chemistry  
15  
16 6 and Chemical Engineering, Hunan University, Changsha, 410082, P.R.China  
17  
18  
19 7

20  
21 8 **Corresponding author: Professor Yuzhi Wang**  
22

23  
24 9 State Key Laboratory of Chemo/Biosensing and Chemometrics  
25

26  
27 10 College of Chemistry and Chemical Engineering  
28

29  
30 11 Hunan University  
31

32  
33 12 Changsha 410082  
34

35  
36 13 P. R. China  
37

38  
39 14 Phone: +86-731-88821903  
40

41  
42 15 Fax: +86-731-88821848  
43

44  
45 16 E-mail: [wyzss@hnu.edu.cn](mailto:wyzss@hnu.edu.cn)  
46  
47  
48  
49  
50  
51  
52  
53  
54  
55  
56  
57  
58  
59  
60

## 23 Abstract

24 A series of hydroxyl ammonium ionic liquids (ILs) have been designed and  
25 synthesized. An ionic liquid aqueous two-phase system (IL-ATPS) based on N,  
26 N-dimethylethanolamine propionate ([DMEA] [Pr]) ionic liquid was studied firstly  
27 for the extraction of proteins. Based on the single-factor experiment, an initial serial  
28 investigative test was used to identify the optimal conditions. Five factors and four  
29 levels orthogonal experiments were used to verify the optimum extraction conditions.  
30 The results showed that under the optimum conditions, the extraction efficiency could  
31 reach up to 99.50%. The RSD of extraction efficiencies in precision experiment,  
32 repeatability experiment and stability experiment were 0.3% (n=5), 1.1% (n=5) and  
33 1.5% (n=5), respectively. The conformation of the proteins was not affected after  
34 extraction into the IL-rich phase in terms of the determination by UV-vis and FT-IR  
35 spectra. According to the determination of conductivity, dynamic light scattering  
36 (DLS), and transmission electron microscope (TEM) images, the microstructure of the  
37 IL-rich phase and the possible mechanism for the extraction were investigated.  
38 Hydrogen bonding interaction, salt out effect and the aggregation phenomenon played  
39 important roles in the extraction. The circular dichroism (CD) spectral experiment  
40 analysis indicated that the secondary structures of the protein were unchanged after  
41 extract. Based on these findings, it is suggested that the method of hydroxyl  
42 ammonium-based ILs- ATPs have the potential to offer new possibility in the  
43 extraction of bio-analysis.

44

1  
2  
3  
4 45 **Key Words:** Hydroxyl ammonium-based ionic liquids, Aqueous two-phase

5  
6 46 system, Protein, Extraction, Circular dichroism.

7  
8  
9 47

10  
11 48

12  
13 49

14  
15  
16 50

17  
18  
19 51

20  
21 52

22  
23 53

24  
25  
26 54

27  
28  
29 55

30  
31 56

32  
33 57

34  
35  
36 58

37  
38  
39 59

40  
41 60

42  
43 61

44  
45  
46 62

47  
48  
49 63

50  
51 64

52  
53 65

54  
55  
56 66

57  
58  
59  
60

## 1. Introduction

Proteins are components of living organism that play critical roles in phenomena like metabolism, gene expression, signal transduction, cellular and extracellular structures, and the like [1]. So, it is particularly necessary to prepare the pure proteins. Proteins always exist within complex mixtures, so centrifugation has been needed to remove bacterial cells in the initial separation step before further purification can be carried out [2,3]. In the past years, the traditional protein purification methods include ion exchange gel filtration chromatography, affinity chromatography [4], membrane separation, ammonium sulfate precipitation, salting out and electrophoresis [5], but they are expensive and not suitable for mass production [6]. Furthermore, due to the poor stability, proteins in the conditions of acids, alkali or heating are easily denatured [7].

Walden was the first one who described the compound ethylammonium nitrate as ionic liquids (ILs) in 1941 [8]. ILs have many fascinating properties including wide liquid ranges, low volatilities (negligible vapor pressure), good thermal stabilities, electrolytic conductivity, wide range of viscosities, adjustable miscibility, reusability, nonflammability and so on [9]. ILs have been widely applied in liquid - liquid extraction of various compounds, such as metal ions [10-13], small organic molecules [14], acids [15], phenols and amines [16,17] and biological compounds, such as proteins [18-23] and DNA [9]. Therefore, ILs have received attention in recent years as “greener solvents” and “designer solvents” [24].

With the beginning of the new century, a new generation of water stable ILs with

1  
2  
3  
4 89 anions like [BF<sub>4</sub>], [PF<sub>6</sub>], [Tf<sub>2</sub>N] or halides were synthesized [25]. Because the strong  
5  
6 90 associative ability of anions within ILs can dissolve proteins, it can lead to the  
7  
8  
9 91 conformational change that can cause destruction [26, 27]. To solve this problem,  
10  
11 92 some water added into the ILs can maintain the activity of the enzyme [28, 29].

12  
13  
14 93 The ionic liquid aqueous two-phase system (IL-ATPS) was reported by Rogers et  
15  
16 94 al [30] for the first time in 2003. IL-ATPS is widely used in the biological separation  
17  
18 95 and purification fields. The aqueous two-phase system formed by inorganic salts  
19  
20 96 usually include poly (ethylene glycol) (PEG) + salt and IL + salt ATPSs. In IL-ATPS,  
21  
22 97 the two phases contain a certain amount of water, and this meets the requirement of  
23  
24 98 the active protein in an ionic liquid solution, which provided a biocompatible  
25  
26 99 environment for the moderate extraction and purification of biological substances. In  
27  
28  
29  
30  
31 100 the previous works, some investigators had studied the extraction of medicinal  
32  
33 101 compounds or proteins by imidazolium [31] or guanidine [7] ionic liquids, but no one  
34  
35  
36 102 had learned the partition of proteins by hydroxyl ammonium ionic liquids.

37  
38  
39 103 Hydroxyl ammonium compounds have attracted widespread concern of the  
40  
41 104 chemist and pharmacologist for the identity of cheap, various form, chemical stability,  
42  
43 105 high catalytic activity and strong physiological activity. Moreover, the hydroxyl  
44  
45 106 ammonium ionic liquid can be synthesized simply by one step with high yields which  
46  
47 107 easy to realize industrial scale production. In recent years, some scientists had studied  
48  
49 108 the applications of hydroxyl ammonium ionic liquids [32] in SO<sub>2</sub> absorption [33],  
50  
51 109 organic synthesis [34] and CO<sub>2</sub> absorption [35].  
52  
53  
54

55  
56 110 The aim of this work is to investigate the partition of proteins in those systems  
57  
58  
59  
60

1  
2  
3  
4 111 based on hydroxyl ammonium IL-ATPS. Such ionic liquids have the similar structure  
5  
6 112 with choline-base ionic liquids which are easy degradable. The concentrations of  
7  
8  
9 113 proteins in top phases were determined by measuring the absorbance at 278 nm for  
10  
11 114 bovine serum albumin (BSA) and ovalbumin (OVA), and at 404 nm for bovine  
12  
13 115 hemoglobin (BHb). BSA was chosen as a model protein to investigate the effect of  
14  
15  
16 116 system parameters and extraction mechanism. Because the synthetic simplicity and  
17  
18  
19 117 low cost of the proposed eight ionic liquids, it is easy to achieve the industrial  
20  
21 118 production scale.  
22  
23  
24 119

## 26 120 **2. Experimental**

### 28 121 **2.1 Apparatus**

30  
31 122 Ionic liquids were dried by a 101-0E Ventilated drying oven (Beijing, China) and  
32  
33 123 DZF-6051 vacuum drying oven (Shanghai, China). A Thermostats cultivating shaker  
34  
35 124 (Shanghai, China) was used to provided a certain temperature and rotation speed in  
36  
37  
38 125 the experiment. A UV-2450 UV-Vis Spectrophotometer (SHIMADZU, Japan) was  
39  
40  
41 126 used to determine the absorbance of the sample.  $^1\text{H}$  NMR spectra were measured with  
42  
43  
44 127 a Varian Inova-400 NMR spectrometer (Varian, USA) at room temperature by using  
45  
46  
47 128 TMS as internal standard. FTIR spectra were recorded on a Spectrum One FTIR  
48  
49 129 Spectrometer (Perkin Elmer, USA). A JEM-3010 transmission electron microscope  
50  
51 130 (JEOL, Japan) was used to examine the microstructures of samples before and after  
52  
53  
54 131 extraction. A DDS-2A conductivity (Shanghai, China) and A ZS-90 dynamic light  
55  
56 132 scattering (Malvern, Britain) were used for the measurement of the mass of ILs and  
57  
58  
59  
60



1  
2  
3  
4 133 sample. Circular Dichroism (CD) spectra were recorded in a MOS-500  
5  
6 134 spectropolarimeter (France).  
7

## 8 9 135 **2.2 Materials and reagents**

10  
11 136 All chemicals used were of analytical grade. Diethyl ethylene diamine (DEEA)  
12  
13 137 was obtained from Aladdin Chemical Reagent Co., Ltd. N, N-dimethylethanolamine  
14  
15 138 (DMEA) were purchased from Tianjin Kermel Fine Chemical Research Institute.  
16  
17 139 Propionic acid (Pr), butanoic acid (Bu), pentanoic acid (Pent), and hexanoic acid  
18  
19 140 (Hex), were all AR grade and purchased from Sinopharm Chemical Reagent Co., Ltd.  
20  
21 141 Bovine serum albumin (BSA), Bovine hemoglobin (BHb) and Ovalbumin (OVA)  
22  
23 142 were all from Sinopharm Chemical Reagent Co., Ltd. Potassium phosphate dibasic  
24  
25 143 anhydrous ( $K_2HPO_4$ ) were purchased from Aladdin Reagents Company (Shanghai,  
26  
27 144 China) and were of 98% purity. Double distilled deionized water was used throughout  
28  
29 145 the experiments.  
30  
31  
32  
33  
34  
35

## 36 146 **2.3 Synthesis and characterization of ILs**

37  
38 147 As we all know, hydroxyl ammonium ionic liquids were synthesized simply by  
39  
40 148 neutralization of the base with the appropriate acid. According to the literature, eight  
41  
42 149 kinds of ILs (as shown in Table 1). By way of example, N,N-dimethylaminoethanol  
43  
44 150 (0.1 mol) dissolved in 10 ml methanol was firstly added to a dried 100ml flask. The  
45  
46 151 flask was equipped with a magnetic stirrer and the temperature was controlled at  
47  
48 152 298.15 K. Propionic acid (0.11mol) was then dropwise added into the flask. After  
49  
50 153 addition was completed within two hours, the solution was stirred at room  
51  
52 154 temperature for 24 h to complete the reaction. Finally, the product was vacuum  
53  
54  
55  
56  
57  
58  
59  
60

1  
2  
3  
4 155 distilled at 50 °C to remove unreacted reactants and the methanol. All the synthetic ILs  
5  
6 156 structures were confirmed by <sup>1</sup>H NMR and FT-IR, which were shown in  
7  
8  
9 157 Supplementary Information Table S1 and Supplementary Information Fig S1  
10  
11 158 respectively.

#### 159 **2.4 Preparation of phase diagram for IL/salt aqueous two-phase systems**

160 The phase diagram for IL/salt aqueous two-phase systems were determined by  
161 the cloud-point method [36]. A few grams of pure ionic liquid were taken into a 10 ml  
162 test tube which contained a number of water. A salt solution of known mass fraction  
163 was added dropwise to the test tube and shaken. After a certain amount of the salt  
164 solution was added, the mixture became turbid or cloudy, and the IL/salt aqueous  
165 two-phase system was formed. Record the volume of the salt solution added. Then the  
166 water was added into the system drop by drop until one further drop made the mixture  
167 clear again, and one phase occurred. The volume of the water added was recorded and  
168 the composition of this mixture was calculated. The above procedure was repeated to  
169 obtain sufficient data to construct the phase diagram. There the X axis was the mass  
170 percentage of the salt solution and the Y axis was the mass percentage of the ILs  
171 solution.

#### 172 **2.5 Protein distribution in Ionic liquid-based aqueous two-phase system**

173 A certain amount of the ionic liquids, K<sub>2</sub>HPO<sub>4</sub> and the solution of proteins were  
174 taken into a 10 mL graduated centrifuge tube. Then the mixture was shaken vigorously  
175 for 20 min to attain equilibrium, and the temperature of the systems was controlled at  
176 278K with a Thermostats cultivating shaker (Shanghai, China). Wait a few minutes in

1  
2  
3  
4 177 order to ensure the formation of two-phase system, then record down the volumes of  
5  
6 178 top phase and bottom phase. After extraction, the top phase solution was taken to  
7  
8  
9 179 determine the concentration of protein after being diluted suitable times. At the same  
10  
11 180 time, the blank experiment was provided to eliminate the other influencing factors in  
12  
13 181 the same condition. Determine the concentration of protein with the external standard  
14  
15 182 method which was measuring the absorbance at 278nm for bovine serum albumin  
16  
17 183 (BSA) and ovalbumin (OVA), and at 404 nm for bovine hemoglobin (BHb) using a  
18  
19 184 UV2450 UV-vis spectrophotometer. The linearity for analyzing BSA, BHb and OVA  
20  
21 185 were in the concentration ranges of 0.05–1.00 mg ml<sup>-1</sup>, 0.025–0.200 mgml<sup>-1</sup> and  
22  
23 186 0.05–1.00 mg ml<sup>-1</sup>, respectively, with correlation coefficients between 0.9998 and  
24  
25 187 0.9999. Partition coefficients (K) of the proteins between the two phases were  
26  
27 188 calculated by the formula :

$$K = C_t / C_b \quad (1)$$

33  
34 189  
35  
36 190 Phase volume ratio (R) is defined as volume ratio of the top phase to the bottom  
37  
38 191 phase:

$$R = V_t / V_b \quad (2)$$

39  
40  
41 192  
42  
43 193 The extraction efficiency (E) was calculated by the following equation:

$$E = C_t V_t / (C_t V_t + C_b V_b) = KR / (1 + KR) \quad (3)$$

44  
45  
46 194  
47  
48 195 C<sub>t</sub> and C<sub>b</sub> are the equilibrium concentrations of the partitioned protein in the IL-rich  
49  
50 196 top phase and the phosphate-rich bottom phase, separately. V<sub>t</sub> and V<sub>b</sub> stand for the  
51  
52 197 volume of the top phase and bottom phase, respectively.  
53  
54  
55

## 56 198 **2.6 Measurement of extraction mechanism**

57  
58  
59  
60

1  
2  
3  
4 199 The conformations of proteins were investigated by UV-vis spectra. BSA in pure  
5  
6 200 water and in IL-rich top phase after extraction were recorded from 200 to 400 nm.  
7

8  
9 201 FT-IR measurements were carried out at room temperature on Perkin-Elmer  
10  
11 202 FT-IR spectrometer (America). FT-IR spectra of pure BSA, pure IL, and BSA in  
12  
13 203 IL-rich top phase were recorded from 4000 to 400  $\text{cm}^{-1}$ .  
14

15  
16 204 Conductivity measurements were performed at 298.15 K by A DDS-2A  
17  
18 205 conductivity (Shanghai, China). The conductance cell was equipped with a water  
19  
20 206 circulating jacketed glass vessel and different concentrations of IL were detected. The  
21  
22 207 uncertainty in conductance measurements was about  $\pm 0.02\%$ .  
23

24  
25  
26 208 The DLS measurements were carried out using a A ZS-90 dynamic light  
27  
28 209 scattering (Malvem, Britain). All measurements were performed at 298.15 K and at  
29  
30 210  $90^\circ$  scattering angle.  
31

32  
33  
34 211 The microscopic structure of the IL-rich top phase is detected by A JEM-3010  
35  
36 212 transmission electron microscope (JEOL, Japan). A carbon Formvar-coated copper  
37  
38 213 grid was laid on a filter paper. One drop of sample solution was dripped on the copper  
39  
40 214 grid as the staining agent and the excess liquid was removed by filter paper. After  
41  
42 215 being dried, the samples were imaged under Vacuum conditions.  
43

## 44 216 **2.7 Determination of the Secondary Structure of protein**

45  
46  
47  
48 217 The circular dichroism of the pure protein and protein in IL-rich top phase after  
49  
50 218 extraction were determined with MOS-500 Circular Dichroism Spectrometer. The  
51  
52 219 concentration of the protein sample was  $0.1\text{mg}\cdot\text{ml}^{-1}$ , cell path was 1 mm, a  
53  
54 220 bandwidth of 2 nm, the range of scan was 190-250 nm and scan speed was  $1\text{ nm}\cdot\text{s}^{-1}$ .  
55  
56  
57  
58  
59  
60

1  
2  
3  
4 221 The sample was scanned for three times and detected at room temperature.  
5

### 6 222 **3. Results and discussion**

#### 7 8 9 223 **3.1 Phase diagrams of ILs**

10  
11 224 As a promising class of new solvents, phase diagram data are required for the  
12  
13 225 design of aqueous two-phase extraction process and for the development of models  
14  
15 226 that predict partitioning of proteins. The binodal curves data determined at 298.15 K  
16  
17 227 and atmospheric pressure for the IL/ $K_2HPO_4$  systems were shown in Fig. 1. These  
18  
19 228 binodal curves can illustrate the information about the concentrations of ILs and salts  
20  
21 229 required to form a two phase systems. As can be seen from these figures, the top  
22  
23 230 phase is IL-rich while the bottom phase is salt-rich. As we all know, for a given salt,  
24  
25 231 the closer the binodal curve is to the origin, the lower the IL concentration required  
26  
27 232 for the formation of two phases. Therefore, it can be seen from Fig. 1 that the ability  
28  
29 233 of the ILs for phase separation follows the order:  
30  
31 234 [DMEA][Pr]<[DMEA][Bu]<[DMEA][Pent]<[DMEA][Hex]<[DEEA][Pr]<[DEEA][  
32  
33 235 Bu]<[DEEA][Pent]<[DEEA][Hex]. Similar trends have been reported in Li et al  
34  
35 236 which reported that hydrophobicity of the ILs could conduce to the higher phase  
36  
37 237 separation capacity [37]. This indicated that [DMEA] [Pr] has the strongest  
38  
39 238 hydrophilic ability above all the ILs in this paper. Considering the fact that  
40  
41 239 [DMEA][Pr],[DMEA][Bu],[DMEA][Pent],[DMEA][Hex],have the same cation but  
42  
43 240 different anions, phase-forming ability of these ILs was determined by the nature of  
44  
45 241 anions. It is easy to see that the ability to form aqueous two-phase is proportional to  
46  
47 242 the anion alkyl chain length. The possible reason is that the more alkyl chain length  
48  
49  
50  
51  
52  
53  
54  
55  
56  
57  
58  
59  
60

1  
2  
3  
4 243 the stronger hydrophobicity, thus decreasing the amount of water available to hydrate  
5  
6 244 ILs. The same principle can be used why the salting-out ability is [DEEA][Pr] >  
7  
8  
9 245 [DMEA][Pr]. By the same token, cation has more impact on the ability to form  
10  
11 246 aqueous two-phase than anion which can be seen from the picture.

12  
13  
14 247 However,  $K_2HPO_4$  was chosen for further study in this work because it not only  
15  
16 248 can configurate ATPS with ILs, but also provide a suitable pH value for the protein  
17  
18  
19 249 extraction in the following study.

## 20 21 250 **3.2 Single factor experiments**

### 22 23 24 251 **3.2.1 Selection of extraction ILs and Protein**

25  
26 252 In order to determine the extraction performance, eight kinds of ionic liquids  
27  
28  
29 253 used in the ATPS have been investigated for the extraction of three proteins namely  
30  
31 254 BSA, BHb and OVA. The extraction efficiencies obtained are given in Table 2 and Fig.  
32  
33  
34 255 2. It can be seen that the different ionic liquids have different abilities to extract  
35  
36 256 various proteins. As an example, the values of the extraction efficiencies for BSA  
37  
38  
39 257 change from 58.69% to 99.47%. This demonstrates that the hydroxyl  
40  
41 258 ammonium-based ILs ATPSs reported here may be a novel option for the purification  
42  
43  
44 259 and separation of biomolecules. Since the [DMEA][Pr] has the highest BSA  
45  
46 260 extraction rate, so the [DMEA][Pr] +  $K_2HPO_4$  ATPSs was chosen in the following  
47  
48  
49 261 experiment.

### 50 51 262 **3.2.2 Effect of the mass of ILs**

52  
53  
54 263 The effect of the amount of added ILs in the systems in which the  
55  
56 264 [DMEA][Pr]/ $K_2HPO_4$  ATPS were used as the extraction system with 2ml (15mg /ml)

1  
2  
3  
4 265 BSA and  $K_2HPO_4$ (1.5g) has been investigated on the extraction efficiency of proteins,  
5  
6 266 which was illustrated in Supplementary Information Table S2 and Fig. 3a. When the  
7  
8  
9 267 IL content varied from 0.9 to 1.0 g, the extraction yield increased rapidly and the  
10  
11 268 highest efficiency was 94.59%. It means that the more the ILs, the more aggregates  
12  
13  
14 269 was formed which facilitated protein extraction. Even if the IL amount increased to  
15  
16 270 2.0 g, the increase of the extraction yield is not obvious. So considering the economic  
17  
18  
19 271 reason 1.0g of ILs for the ATPS was chosen in next experiment.

### 20 21 272 **3.2.3 Effect of the mass of $K_2HPO_4$**

22  
23  
24 273 As an example, the effect on BSA distribution of the mass of  $K_2HPO_4$  was  
25  
26 274 studied, and the results were illustrated in Fig. 3b. As indicated in this figure, the  
27  
28  
29 275 extraction efficiency changes with the various concentrations of  $K_2HPO_4$  over the  
30  
31 276 range of 1.4-3 g. With the increase of the amount of salt, the extraction efficiency of  
32  
33  
34 277 BSA was up to 98.97%. So the phenomenon indicated that the salt out effect was the  
35  
36 278 driving force for the protein extraction. However, the extraction efficiency decreases  
37  
38  
39 279 rapidly when the salt mass is greater than 2.0g. The cause maybe that with the salt  
40  
41 280 concentration increasing, the more water transferred from top phase to bottle phase  
42  
43  
44 281 then leads to reduce water content of IL. As the bottle phase is highly hydrophilic than  
45  
46 282 the top phase, the hydrogen bonding interaction between the surface water of protein  
47  
48  
49 283 and amino acid residue is more easier for protein to transfer into salt- rich phase. It is  
50  
51 284 obvious that salt out effect and hydrogen bonding interaction act as a combined effect  
52  
53  
54 285 for protein extraction. Therefore, the salt mass was determined as 2.0 g for the next  
55  
56 286 experiments.  
57  
58  
59  
60

### 287 **3.2.4 Effect of the mass of BSA**

288 In order to find the optimum content of BSA studied on the influence of  
289 extraction efficiency, different concentrations of protein was adopted and the results  
290 were illustrated in Fig. 3c. It is clear that the extraction efficiency was increased with  
291 the increasing of the mass of BSA between 5mg-10mg and when the mass of BSA  
292 was higher than 10mg, the extraction efficiency had fallen rapidly. This may be  
293 because the extraction system has a limited ability of extraction with a certain amount  
294 of ionic liquid. So with the protein increases, the extraction efficiency were continue  
295 to reduce. The equilibrium concentrations of the partitioned protein in the IL-rich top  
296 phase and the phosphate-rich bottom phase were constantly changed, so the K was  
297 also changed. According to the above result, 10 mg BSA was selected for further  
298 experiment.

### 299 **3.2.5 Effect of the separation time**

300 The effect of the extraction time in IL-based ATPS was investigated by changing  
301 the shaking time of the IL-based ATPS. 1g [DMEA][Pr] and 2g K<sub>2</sub>HPO<sub>4</sub> and 2ml of  
302 5mg/ml BSA were added into a series of the test tubes which were shaken at 200 rpm  
303 for different shaking time periods of 2, 4, 8, 10, 15, 20, 25, 30 min and the time  
304 dependence of the extraction efficiency was illustrated in Fig. 3d. It can be seen that  
305 with the increase of the shaking time the extraction yield of BSA obviously increased  
306 from 68.29% to 99.24% in the range of 2-20 min. And when separation time was  
307 increased to 30 min, the extraction efficiency was keeping an extraction efficiency of  
308 almost 99.50% and reached the equilibrium. Therefore, 20 min was chosen as the



1  
2  
3  
4 309 shaking time for the extraction.  
5

### 6 310 **3.2.6 Effect of the temperature** 7

8  
9 311 To further confirm the extraction temperature studied on the influence of  
10  
11 312 extraction efficiency of BSA in IL-based aqueous two-phase systems, the BSA  
12  
13 313 content on its distribution behavior was also studied. In light of Fig. 3e, as the  
14  
15 314 temperature increased from 15 to 25 °C, the extraction efficiency of the protein  
16  
17 315 increased from 86.59% to 99.24%. When the temperature kept at 30 °C or higher, the  
18  
19 316 extraction yield decreased correspondingly. The possible reason for this phenomenon  
20  
21 317 was that the increased extraction temperature could reduce the viscosity of the ionic  
22  
23 318 liquid, enhance the solvent solubility and diffusion capacity. But when the  
24  
25 319 temperature continues to rise, the extraction rate was reduced. On the one hand, it  
26  
27 320 means that the temperature was high to destroy the hydrogen bonding interaction  
28  
29 321 between the surface water of protein and amino acid residue. On the other hand, as the  
30  
31 322 temperature rises, the extraction rate is reduced resulting in a tendency for the liquid  
32  
33 323 homogeneous. Through further study found that when the temperature exceeds 60 °C,  
34  
35 324 BSA was denaturated. So the extraction was carried out at 25 °C because of the  
36  
37 325 relatively high extraction yield.  
38  
39  
40  
41  
42  
43  
44  
45

### 46 326 **3.3 Orthogonal experiment** 47

48  
49 327 As a promising class of new solvents, the optimize conditions were determined  
50  
51 328 through an orthogonal array experimental design  $L_{16}(4^5)$  by mass of IL (factor A),  
52  
53 329 mass of  $K_2HPO_4$  (factor B), concentration of BSA (factor C), temperature (factor D)  
54  
55 330 and separation time (factor E). An  $L_{16}(4^5)$  matrix, which is an orthogonal array of five  
56  
57  
58  
59  
60

1  
2  
3  
4 331 factors and four levels was employed to assign the considered factors and levels (as  
5  
6 332 shown in Table 3). K1, K2, K3 and K4 mean the average extraction efficiencies of  
7  
8  
9 333 each factor in each of the level. The bigger the difference of R is, the more influence  
10  
11 334 the factor has on the extraction efficiency which R was determined by the difference  
12  
13  
14 335 value between the maximum and minimum values of K. The results show that the  
15  
16 336 impact of various factors on the importance of the extraction efficiency were:  
17  
18  
19 337  $A > B > E > C > D$ , and the optimize conditions are  $A_4B_4C_2D_3E_3$  by 99.62% of the  
20  
21 338 extraction efficiency.

### 22 23 24 339 **3.4 Method validation**

25  
26 340 At the optimal conditions, the ILs-ATPS were composed by 1.0 g of IL, 2.0g of  
27  
28 341  $K_2HPO_4$  and 2 ml of 5.0 mg/ml BSA which were validated by the precision  
29  
30 342 experiment, repeatability experiment and stability experiment ( as shown in  
31  
32  
33 343 Supplementary Information Table S3). Apparatus precision was investigated by the  
34  
35  
36 344 analysis of the top phase of the solution of BSA for five times by UV detection. The  
37  
38  
39 345 RSD obtained was 0.3%.The result indicates that the precision of the UV-vis spectra  
40  
41 346 is great. Five copies of the same sample measured respectively under the same  
42  
43  
44 347 conditions. The calculation of RSD was 1.1% (n=5) which indicate that this method  
45  
46 348 has excellent repeatability. Taking a sample detected continuously in five days under  
47  
48  
49 349 the same conditions to verify the stability experiment. The result of the relative  
50  
51 350 standard deviation (RSD) of extraction efficiency was 1.5% (n=5), which explain that  
52  
53  
54 351 the sample is recoverable within five days.

### 55 56 352 **3.5 Extraction mechanism**

57  
58  
59  
60

### 353 3.5.1 UV-Vis spectroscopy

354 UV-vis spectra were investigated for BSA in order to examine the conformation  
355 of proteins before and after extraction. The UV-vis spectra of BSA in pure water and  
356 in IL-rich top phase after extraction were shown in Fig. 4. It is obvious that the  
357 UV-vis spectra of BSA are similar and its maximum absorption is at the same  
358 position (at 278 nm) in pure water and in the [DMEA][Pr]-rich upper phase after  
359 extraction. This explains that there are no direct chemical bonds interactions between  
360 BSA molecules and the ILs in the extraction process which further confirmed that the  
361 spatial structure of the protein was not destroyed.

### 362 3.5.2 FT-IR spectroscopy

363 FT-IR spectroscopy is one of the common experimental methods recognized as  
364 useful in providing information on structure features of compounds or chemical bonds  
365 in a molecule or an interaction system, attributable to the unique energy absorption  
366 bands for specific bonding environments or interactions [38]. As is known, proteins  
367 are irregular polymers made up essentially of 20 amino acids with four levels of  
368 spatial structure. Amide is the basic unit of the peptide bond: amide I is assigned to  
369 both C=O stretching vibration and ring stretching vibrations, while amide II is  
370 assigned to C-N stretching vibrations [7]. The absorption bands most widely used as  
371 structure probes in protein FT-IR spectroscopy have been the amide I vibrations (1690  
372  $-1600\text{cm}^{-1}$ ) and amide II stretching vibrations (1600-1500) [39]. Fig. 5 showed the  
373 FT-IR spectra of pure BSA, pure IL, and BSA in IL. It was found that the amide I  
374 bond (at  $1655\text{ cm}^{-1}$ ) and amide II band (at  $1550\text{ cm}^{-1}$ ) shown the characteristics of the

1  
2  
3  
4 375 BSA. From Fig. 5B, the two characteristics of the BSA absorption bands have  
5  
6 376 remained in the similar region after extraction in the IL-BSA complexity. It can be  
7  
8  
9 377 seen that the conformation of the protein was not changed in the IL phase and no new  
10  
11 378 chemical bonds generated which was further confirmed the conclusion with UV-vis  
12  
13 379 detection. By the way, the  $3237\text{ cm}^{-1}$  was assigned to both N-H and O-H stretching  
14  
15  
16 380 vibration of hydroxyl ammonium ionic liquid which illustrated that the hydroxyl  
17  
18  
19 381 ammonium ionic liquids could exist in a large number of hydroxyl groups with  
20  
21 382 proteins to form intermolecular hydrogen bonds. Therefore hydroxyl ammonium  
22  
23  
24 383 IL-based aqueous two-phase extraction systems have great potential applications in  
25  
26 384 purification of biological macromolecules.

### 28 385 **3.5.3 Conductivity and DLS detection.**

31 386 The conductivity was measured at 298.15 K with different concentrations of IL  
32  
33  
34 387 solution. The conductivities exhibit typical behavior with two linear fragments, and  
35  
36 388 the concentration at which the two linear fragments intersect is assigned to the critical  
37  
38  
39 389 aggregation concentration (CAC)[7].Fig. 6a shows the CAC value of the [DMEA][Pr]  
40  
41 390 was 0.13 g/ ml which was lower than the top phase of the ATPS investigated in the  
42  
43  
44 391 present work. It is illustrated that the IL aggregates were formed with BSA in the top  
45  
46 392 phase.

48  
49 393 Fig. 6b-d shows the DLS results of the aqueous protein solution and aqueous  
50  
51 394 IL+ protein solution. A new and intensity aggregation emerged in the range of  
52  
53  
54 395 100–1000 nm, which was larger than the aggregation of the pure protein. This is  
55  
56 396 because the interaction may occur between the ionic liquid and the protein which  
57  
58  
59  
60

1  
2  
3  
4 397 illustrates that the formation of aggregates is one of the main driving forces in the  
5  
6 398 extraction of protein by IL-ATPS. As shown in Fig.6d, another intensity aggregation  
7  
8  
9 399 emerged in the range of 1000–10000 nm in the top phase of the ATPS with BSA  
10  
11 400 added which may be the formation of aggregates by the excess ionic liquids and the  
12  
13  
14 401 intensity of the aggregation is less than that shown in Fig. 6b.

#### 15 16 402 **3.5.4 Detection of the microscopic structure of IL-rich top phase by TEM**

17  
18  
19 403 The microscopic structure of the IL-rich top phase is detected by transmission  
20  
21 404 electron microscopy for a further understanding of the separation process. Fig. 7a  
22  
23 405 shows the conformation of IL-rich top phase without protein and the spot may be the  
24  
25  
26 406 ionic liquid without too much aggregation. Fig. 7b shows the appearance of pure  
27  
28  
29 407 protein and Fig. 7c-d show the distribution of IL-rich top phase after extract protein.  
30  
31 408 From the TEM images it can be seen that the IL-aggregate-protein complex was taken  
32  
33  
34 409 shape after the BSA was extracted in the top phase. The results test by TEM  
35  
36  
37 410 consistent with DLS. That is to say, the aggregation was the main driving force of  
38  
39 411 protein partitioning in an ionic liquid-based aqueous two-phase system.

#### 40 41 412 **3.6 Analysis of the Secondary Structure of protein**

42  
43 413 Far-ultraviolet circular dichroism (CD) can reflect the secondary structure of a  
44  
45 414 protein from 190 to 250 nm. The characteristic of the  $\alpha$ -helix structure of protein  
46  
47 415 shows a positive band centered at 192 nm and two negative bands centered at 208 and  
48  
49  
50 416 222 nm. The  $\beta$ -sheet structure of protein shows a negative band centered at 216 nm.  
51  
52  
53 417 Fig. 8 shows the circular dichroism spectra of the pure BSA in water and BSA in  
54  
55 418 IL-rich phase. The main observed spectral characteristic of BSA CD curve almost  
56  
57  
58 419 kept the same. The result demonstrated that the secondary structure of the protein was

1  
2  
3  
4 420 unchanged after extraction by ionic liquid. In other words, hydroxyl ammonium ionic  
5  
6 421 liquid aqueous two-phase extraction systems provide a gentle environment for protein  
7  
8  
9 422 extraction.

#### 423 **4. Conclusions**

424 This paper systematically investigated the extraction efficiency of protein in  
425 hydroxyl ammonium ionic liquid/ $K_2HPO_4$  of aqueous two-phase system. In  
426 comparison with the references reported method, the greatest benefit of the present  
427 method is that the adapted extraction solvent is timesaving (just 20 min in this study),  
428 cost saving (the synthetic materials of hydroxyl ammonium-based ionic liquid are  
429 abundant-sourced and low-cost), and also easy to achieve industrial scale production.  
430 Moreover, such ionic liquids are green and environmentally friendly because they  
431 have similarities structural with choline-base ionic liquids which are easy degradable.  
432 The high extraction rate (99.50%) illustrate that the proposed method of hydroxyl  
433 ammonium ILs-based ATPs for the selective separation of protein would have  
434 potential applications in bio-analysis and bio-separation. UV-vis and FT-IR spectra  
435 were investigated for BSA in order to examine the conformation of proteins before  
436 and after extraction. The determination of conductivity, DLS and TEM determinations  
437 proved that the hydrogen bonding interaction, salt out effect and the aggregation  
438 phenomenon played important roles in the extraction. The result of CD provides  
439 useful information for analyzing the advanced structure of the protein after extraction  
440 by ionic liquid.

441

442 **Acknowledgements**

443 The authors greatly appreciate the financial supports by the National Natural  
444 Science Foundation of China (No. 21175040; No.21375035; No.J1210040) and the  
445 Foundation for Innovative Research Groups of NSFC (Grant 21221003).

446 **References**

- 447 [1] Y. C. Pei, J. J. Wang, *Separation and Purification Technology*, 2009, **64**, 288-295.
- 448 [2] L. Xiao, Y. Z. Wang, *Analyst*, 2013, **138**, 6445-6453.
- 449 [3] T. Oshima, H. Higuchi, K. Ohto, K. Inoue, M. Goto, *Langmuir*, 2005, **21**, 7280-7284.
- 450 [4] K. E. Gutowski, G. A. Broker, H. D. Willauer, J. G. Huddleston, R. P. Swatloski, J. D. Holbrey  
451 and R. D. Rogers, *J. Am. Chem. Soc.*, 2003, **125**, 6632-6633.
- 452 [5] M. G. Freire, A. F. M. Cláudio, J. M. M. Araújo, J. A. P. Coutinho, I. M. Marrucho, J. N.  
453 Canongia Lopes and L. P. N. Rebelo, *Chem. Soc. 70 Rev.*, 2012, **41**, 4966-4995.
- 454 [6] S. Shahriari, L. C. Tome, J. M. M. Araujo, L. P. N. Rebelo, *RSC Advance*, 2013, **3**, 1835-1843.
- 455 [7] Q. Zeng, Y. Z. Wang, *Talanta*, 2013, **116**, 409-416.
- 456 [8] P. Walden, *Bull Acad Imperial Sci*, 1914, **1800**, 405-422.
- 457 [9] P. Sun, D. W. Armstrong, *Analytica Chimica Acta*, 2010, **661**, 1-6.
- 458 [10] N. Hirayama, H. Okamura, K. Kidani, H. Imura, *Analytical Sciences Anal*, 2008, **24**, 697-699.
- 459 [11] K. Shimojo, M. Goto, *Analytical chemistry*, 2004, **76**, 5039-5044.
- 460 [12] K. Kidani, N. Hirayama, H. Imura, *Analytical Sciences Anal*, 2008, **24**, 1251-1256.
- 461 [13] G. Wei, Z. Yang, C. Lee, H. Yang, C.R.C. Wang, *J. Am. Chem. Soc.*, 2004, **126**, 5036-5037.
- 462 [14] L. G. Abreu, V. Pino, A. M. Afonso, *Journal of Chromatography A*, 2008, **1214**, 23-29.
- 463 [15] G. Absalan, M. Akhond, L. Sheikhan, *Talanta*, 2008, **77**, 407-411.

- 1  
2  
3  
4 464 [16] V. M. Egorov, S. V. Smirnova, I. V. Pletnev, *Sep. Purif. Technol*, 2008, **63**, 710–718.  
5  
6 465 [17] Y. Lu, W. Ma, R. Hu, X. Dai, Y. Pan, *Journal of Chromatography*, 2008, **1208**, 42–46.  
7  
8 466 [18] Y. Pei, J. Wang, K. Wu, X. Xuan, X. Lu, *Sep. Purif. Technol*, 2009, **64**, 288–292.  
9  
10 467 [19] S. Kamran, M. Asadi, G. Absalan, *Microchim Acta*, 2013, **180**, 41–48.  
11  
12 468 [20] Z. Du, J. J. Wang, *Chemistry A European Journal*, 2007, **13**, 213-2137.  
13  
14 469 [21] S. Dreyer, U. Kragl, *Biotechnology and Bioengineering*, 2008, **99**, 1416-1424.  
15  
16 470 [22] K. E. Goklena and T. A. Hatton, 2012, **22**, 831-841.  
17  
18 471 [23] M. Erbedinger, A. J. Mesiano, A. J. Russell, 2000, **16**, 1129-1131.  
19  
20 472 [24] G. A. Baker, S. N. Baker, S. Pandey, F. V. Bright, *Analyst*, 2005, **130**, 800–808.  
21  
22 473 [25] S. Oppermann, F. Stein, U. Kragl, *Appl Microbiol Biotechnol*, 2011, **89**, 493–499.  
23  
24 474 [26] W. Y. Lou, M. H. Zong, T. J. Smith, H. Wu and J. F. Wang, *Green Chem*, 2006, **8**, 509–512.  
25  
26 475 [27] S. Cantone, U. Hanefeld and A. Basso, *Green Chem*, 2007, **9**, 954–971.  
27  
28 476 [28] S. N. Baker, S. Pandey and G. A. Baker, *Chem. Commun*, 2004, **43**, 940–941.  
29  
30 477 [29] T. De Diego, P. Lozano and J. L. Iborra, *Biomacromolecules*, 2005, **6**, 1457–1464.  
31  
32 478 [30] K. E Gutowski, G. A. Broker, R. D. Rogers, *J Am Chem Soc*, 2003, **125**, 6632–6633.  
33  
34 479 [31] Y. Yuan, Y. Wang, R. Xu, M. Huang and H. Zeng, *Analyst*, 2011, **136**, 2305–2312.  
35  
36 480 [32] J. L. C. Anabela, K. Shimizu, M. M. Isabel, *Chem Phys Chem*, 2012, **13**, 1902–1909.  
37  
38 481 [33] K. Huang, X. B. Hu, Z. B. Zhang, *Chemical Engineering Journal*, 2013, **215**, 36–44.  
39  
40 482 [34] A. L. Zhu, R. X. Liu, L. J. Li, L. Wang, J. J. Wang, *Catalysis Today*, 2013, **200**, 17–23.  
41  
42 483 [35] K. A. Kurnia, F. Harris, C.D. Wilfred, *J. Chem. Thermodynamics*, 2009, **41**, 1069–1073.  
43  
44 484 [36] S. Li, C. He, K. Li and F. Liu, *Journal of Chromatography B*, 2005, **826**, 58–62.  
45  
46 485 [37] S. Li, C. He, H. Liu, K. Li, F. Liu, *Journal of Chromatography B*, 2005, **826**, 42–46.  
47  
48  
49  
50  
51  
52  
53  
54  
55  
56  
57  
58  
59  
60



1  
2  
3  
4 486 [38] L. Jin, R. B. Bai, *Langmuir*, 2002, **18**, 9770–9778.  
5

6 487 [39] J. W. Brauner, C. R. Flach, R. Mendelsohn, *J. Am. Chem. Soc.*, 2005, **127**, 109–115.  
7

8 488

9 489

10 490

11 491

12 492

13 493

14 494

15 495

16 496

17 497

18 498

19 499

20 500

21 501

22 502

23 503

24 504

25 505

26 506

27 507

28 508

29 509

30 510

31 511

32 512

33 513

34 514

35 515

36 516

37 517

38 518

39 519

40 520

41 521

42 522

43 523

44 524

45 525

46 526

47 527

48

49

50

51

52

53

54

55

56

57

58

59

60

528

529

Table 1 The structures of eight ILs

ILs	Cation	Anion
[DMEA][Pr]		
[DMEA][Bu]		
[DMEA][Pent]		
[DMEA][Hex]		
[DEEA][Pr]		
[DEEA][Bu]		
[DEEA][Pent]		
[DEEA][Hex]		

530

531

532

533

534

535 **Table 2.**The extraction efficiencies of proteins by ATPSs based on ionic liquids (5.0mmol),  
 536 **and K<sub>2</sub>HPO<sub>4</sub> (1.5g) solutions and Protein (15mg/ml, 2.0mL). (n=3)**

Ionic liquid	Efficiency (%)		
	Bovine serum albumin	Bovine hemoglobin	Ovalbumin
[DMEA][Pr]	99.47	18.11	68.02
[DMEA][Bu]	95.87	20.09	63.69
[DMEA][Pent]	93.09	52.54	51.07
[DMEA][Hex]	64.80	60.64	51.69
[DEEA][Pr]	89.43	32.53	36.37
[DEEA][Bu]	88.50	47.32	38.80
[DEEA][Pent]	61.44	54.91	43.48
[DEEA][Hex]	58.70	59.01	39.17

537  
 538 Note: 1. E% was represented the extraction efficiency, which was calculated from  
 539 equation (3).  
 540  
 541  
 542  
 543  
 544  
 545  
 546  
 547  
 548  
 549  
 550  
 551  
 552  
 553  
 554  
 555  
 556  
 557

558 Table 3. Results of orthogonal experiment L<sub>16</sub> (4<sup>5</sup>)

Experiment	A IL(g)	B salt(g)	C BSA(mg)	D T(□)	E t(min)	E(%)
1	1(0.8)	1(1.6)	1(5)	1(15)	1(15)	79.51
2	1	2(1.8)	2(10)	2(20)	2(20)	90.21
3	1	3(2)	3(15)	3(25)	3(25)	91.05
4	1	4(2.2)	4(20)	4(30)	4(30)	90.27
5	2(1)	1	2	3	4	94.54
6	2	2	1	4	3	97.10
7	2	3	4	1	2	97.35
8	2	4	3	2	1	95.74
9	3(1.8)	1	3	4	2	88.83
10	3	2	4	3	1	91.37
11	3	3	1	2	4	92.16
12	3	4	2	1	3	99.71
13	4(1.6)	1	4	2	3	94.91
14	4	2	3	1	4	93.05
15	4	3	2	4	1	98.57
16	4	4	1	3	2	99.86
K1	87.76	89.45	92.16	92.40	91.30	major and minor order: A>B>E>C>D optimize conditions:A <sub>4</sub> B <sub>4</sub> C <sub>2</sub> D <sub>3</sub> E <sub>3</sub>
K2	91.52	92.93	95.76	93.25	93.17	
K3	93.24	94.78	92.17	94.20	95.69	
K4	94.82	96.39	93.48	93.69	92.50	
R	7.06	6.94	3.60	1.80	4.40	
Optimal level	A <sub>4</sub>	B <sub>4</sub>	C <sub>2</sub>	D <sub>3</sub>	E <sub>3</sub>	

559

560

1  
2  
3 **561 Figure captions**

4  
5 562 Fig. 1. Phase diagram of IL/salt aqueous two-phase systems

6  
7 563 Fig. 2. Effect of kinds of IL for extraction different protein

8  
9  
10 564 Fig. 3. Single factor effect of protein extraction: mass of IL (a), mass of  $K_2HPO_4$  (b),  
11  
12 mass of BSA (c), separation time (d), temperature (e).

13  
14 565  
15 566 Fig. 4. UV-vis spectra of BSA in pure water and in IL-rich top phase after extraction.

16  
17 567 Fig. 5. FT-IR spectra of pure [DMEA][Pr], pure BSA and BSA in [DMEA][Pr]. (a)

18  
19 568 pure [DMEA][Pr]; (b) pure BSA; (c) BSA in IL-rich top phase.

20  
21 569 Fig. 6. The aggregates size distribution: (a) Concentration dependence of the

22  
23 570 conductivity for [DMEA][Pr] in aqueous solutions at 25 °C. (b) IL in pure water.

24  
25 571 (c) BSA in pure water. (d) Size distribution of the top phase of the ATPS with

26  
27 572 BSA added.

28  
29 573 Fig. 7. TEM images of the aggregates: (a) ILs-ATPS without BSA. (b) Pure BSA. (c,

30  
31 574 d) Image of the top phase of the ATPS with BSA added.

32  
33 575 Fig. 8. Circular dichroism spectra of BSA in pure water and in IL-rich top phase after

34  
35 576 extraction.

36  
37 577 Fig. S1 Infrared spectroscopy of ILs: a. [DMEA][Pr], b. [DMEA][Bu], c.

38  
39 578 [DMEA][Pent], d. [DMEA][Hex], e. [DEEA][Pr], f. [DEEA][Bu], g.

40  
41 579 [DEEA][Pent], h. [DEEA][Hex].

42  
43 580

44  
45 581

46  
47

48  
49

50  
51

52  
53

54  
55

56  
57

58  
59

60

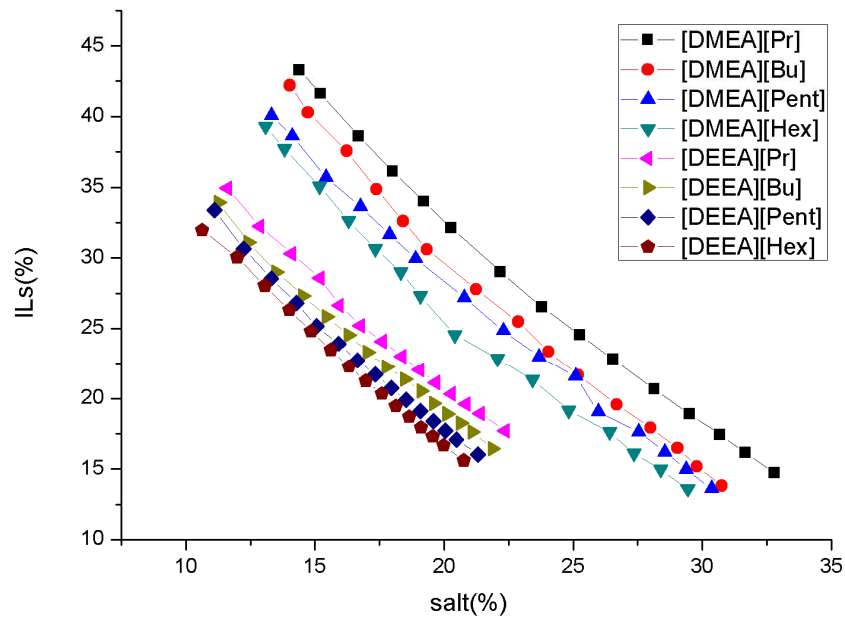
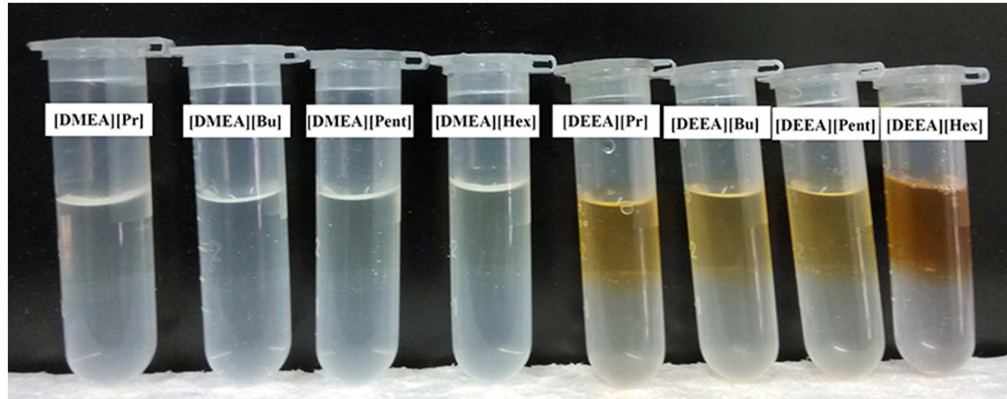
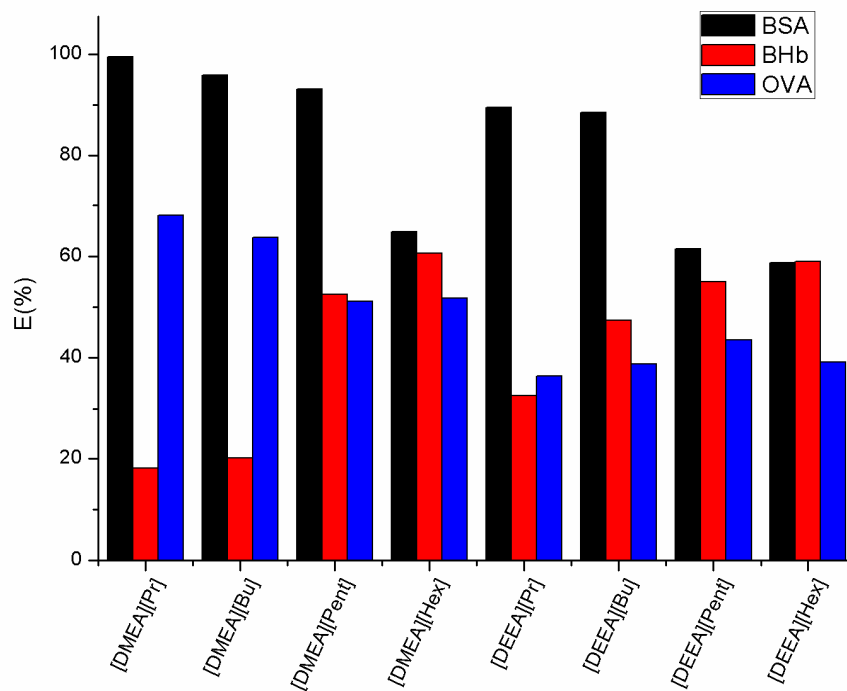


Fig. 1. Phase diagram of IL/salt aqueous two-phase systems

582  
583  
584  
585  
586  
587  
588  
589  
590  
591  
592  
593  
594  
595  
596  
597  
598



599

600

601 Fig. 2. Effect of kinds of IL for extraction different protein

602

603

604

605

606

607

608

609

610

611

612

613

614

615

616

617

618

619

620

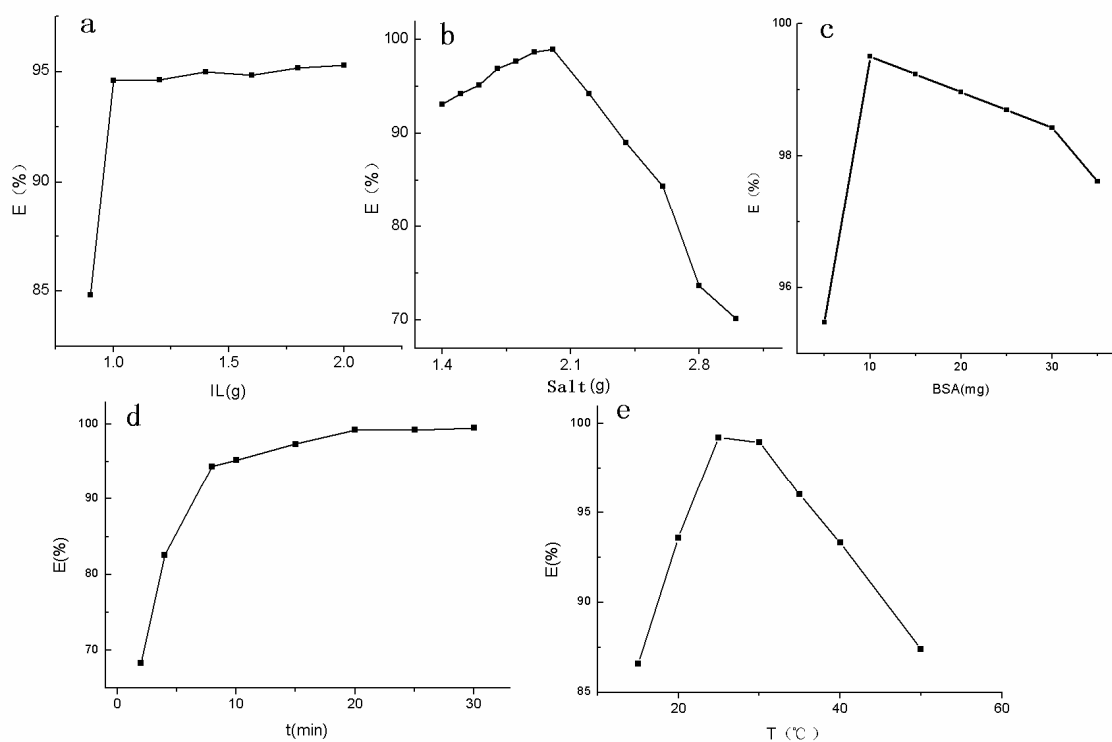


Fig. 3. Single factor effect of protein extraction: mass of IL (a), mass of  $K_2HPO_4$  (b), mass of BSA (c), separation time (d), temperature (e).

621  
622  
623  
624  
625  
626  
627  
628  
629  
630  
631  
632  
633  
634  
635  
636  
637  
638  
639  
640  
641  
642  
643  
644



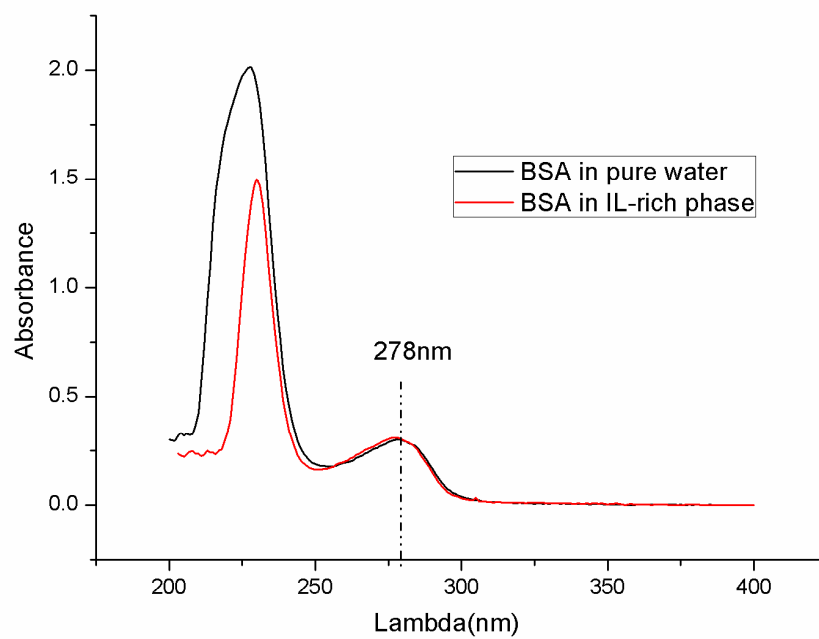
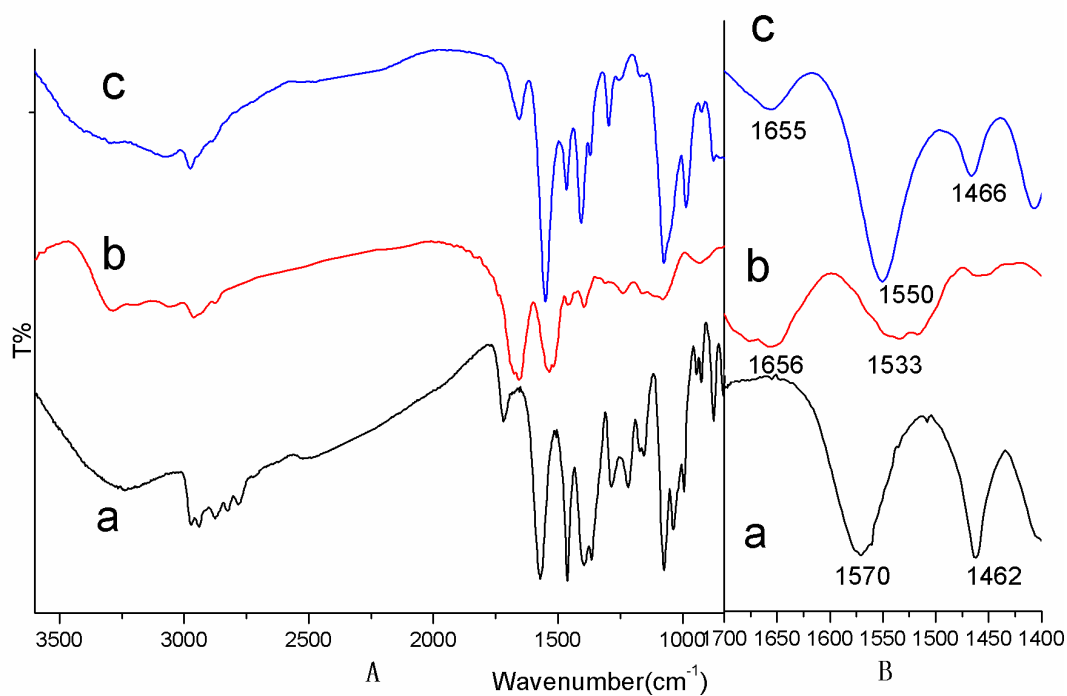


Fig. 4. UV-vis spectra of BSA in pure water and in IL-rich top phase after extraction.



670

671

672 Fig. 5. FT-IR spectra of pure [DMEA][Pr], pure BSA and BSA in [DMEA][Pr]. (a)  
673 pure [DMEA][Pr]; (b) pure BSA; (c) BSA in IL-rich top phase.

674

675

676

677

678

679

680

681

682

683

684

685

686

687

688

689

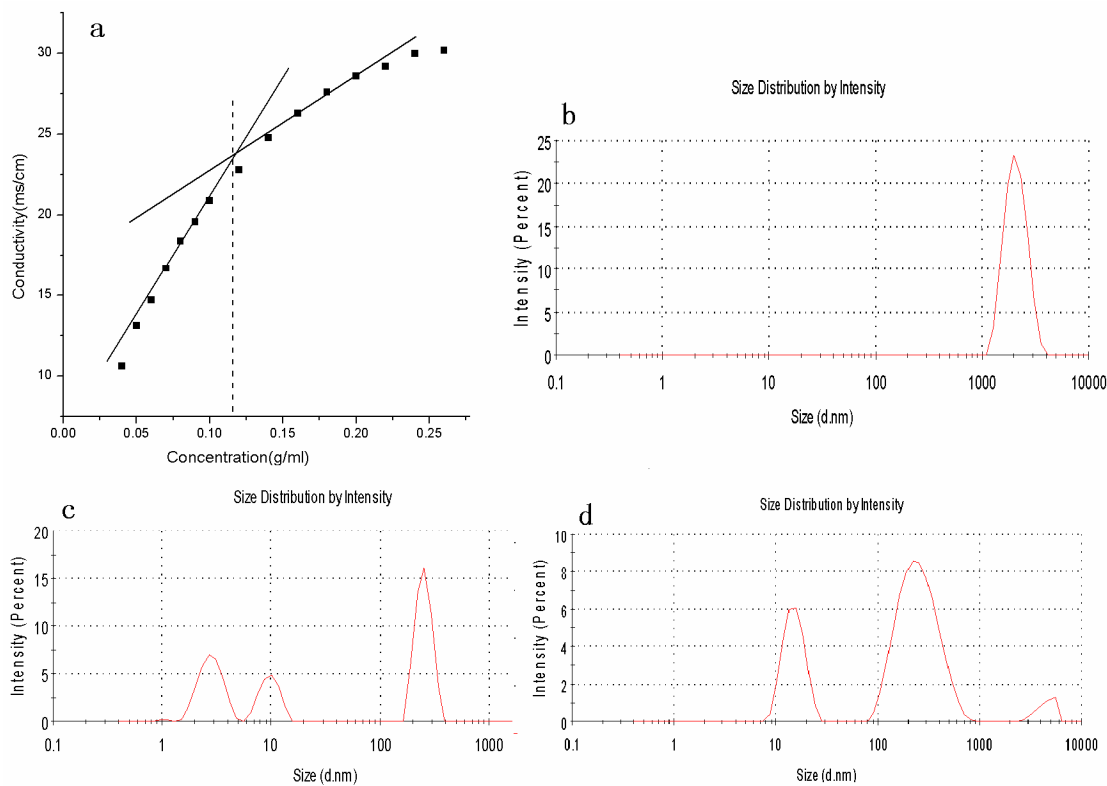
690

691

692

693

694



695

696

697 Fig. 6. The aggregates size distribution:(a)Concentration dependence of the

698 conductivity for [DMEA][Pr] in aqueous solutions at 25°C. (b) IL in pure water. (c)

699 BSA in pure water. (d) Size distribution of the top phase of the ATPS with BSA

700 added.

701

702

703

704

705

706

707

708

709

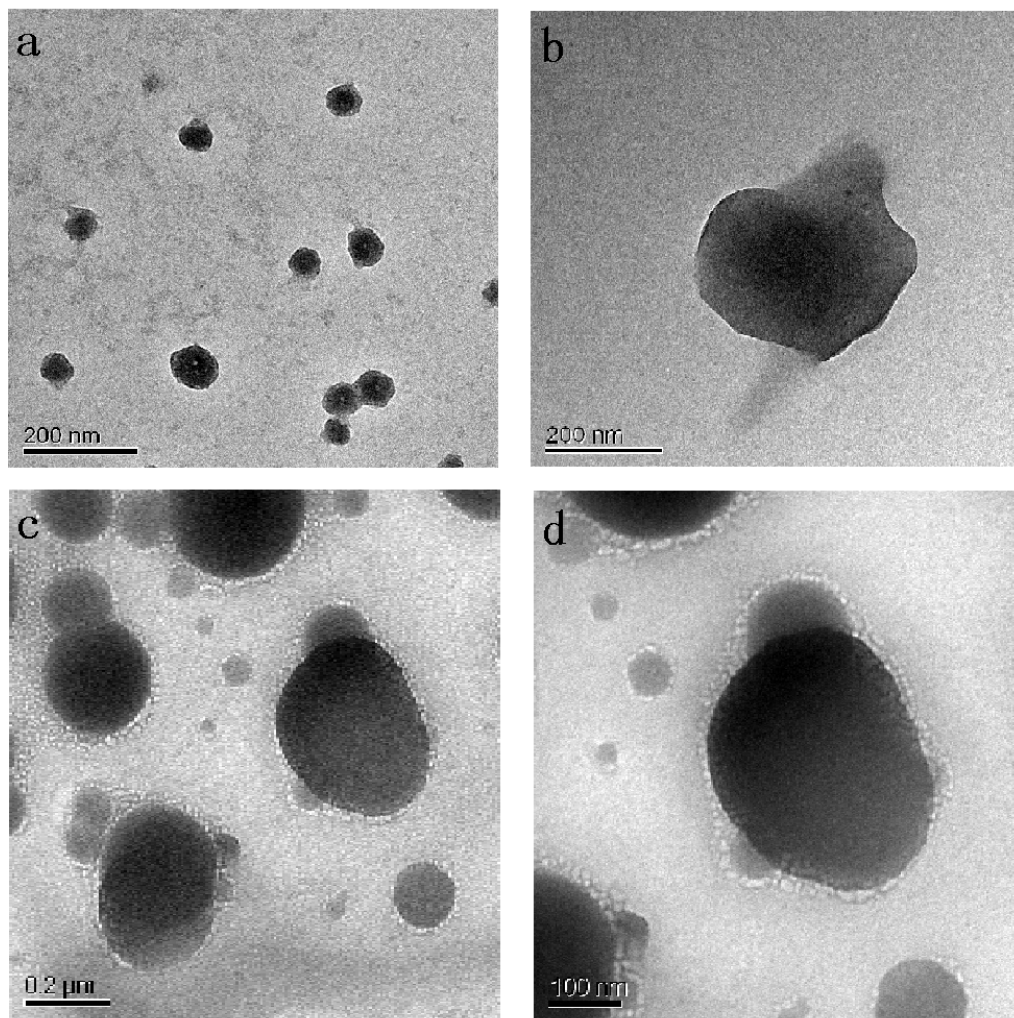
710

711

712

713

714



715

716

717 Fig. 7. TEM images of the aggregates: (a) ILs-ATPS without BSA. (b) Pure BSA. (c,

718 d) Image of the top phase of the ATPS with BSA added.

719

720

721

722

723

724

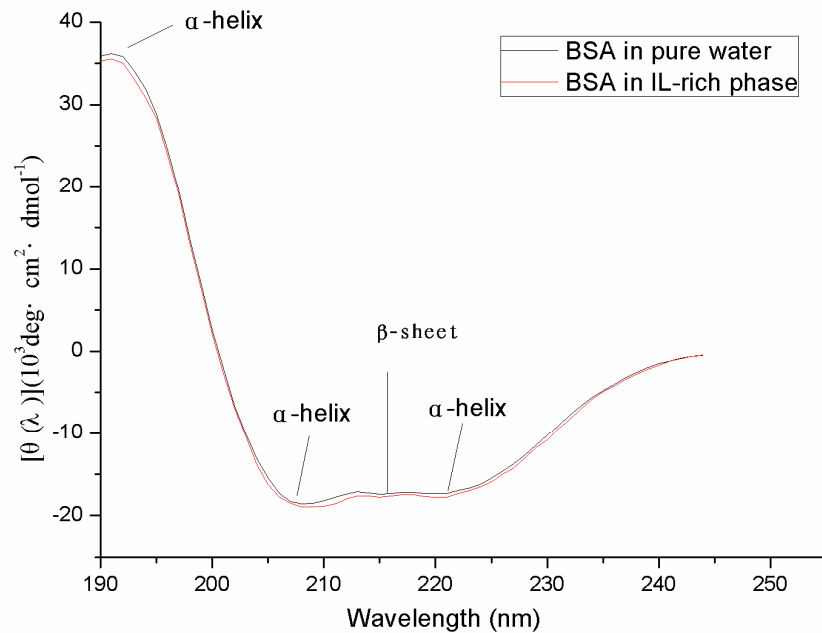
725

726

727

728

729



730

731 Fig. 8. Circular dichroism spectra of BSA in pure water and in IL-rich top phase after  
732 extraction.

733

734

735

736

737

738

739

740

741

742

743

744

745

746

747

748

749

750

751

752